Optical shielding of cold collisions in blue-detuned near-resonant optical lattices

J. Piilo[1] and K.-A. Suominen[1,2]
[1]*Helsinki Institute of Physics, PL 64, FIN-00014 Helsingin yliopisto, Finland*
[2]*Department of Physics, University of Turku, FIN-20014 Turun yliopisto, Finland*
(Received 14 February 2002; published 1 July 2002)

We report Monte Carlo wave-function simulation results for two colliding atoms in a blue-detuned near-resonant $J=1\rightarrow J=1$ optical lattice. Our results show that complete optical shielding of collisions can be achieved within the lattice with suitably selected and realistic laser field parameters. More importantly, our results demonstrate that the shielding effect does not interfere with the actual trapping and cooling process, and it is produced by the lattice lasers themselves, without the need to use additional laser beams.

DOI: 10.1103/PhysRevA.66.013401 PACS number(s): 32.80.Pj, 34.50.Rk, 42.50.Vk, 03.65.−w

I. INTRODUCTION

In laser cooling and trapping of neutral atoms, spatial variations in the polarization and intensity of light can be effectively turned into potentials for atoms [1]. Optical lattices are an important application of this technique [2]. By using suitable laser field configurations and parameters, one can achieve localization of atoms into lattice sites, at least for some period of time on average. In practice, there are two distinct cases of optical lattices. For near-resonant light the lasers are responsible for both cooling and trapping of atoms, usually achieved by a strong scattering of photons (energy dissipation). The basic example is the Sisyphus or polarization gradient cooling mechanism [3]. In contrast, with far off-resonant light we obtain only a conservative lattice potential without the cooling mechanism, with a strong reduction in photon scattering. This allows many delicate experiments involving quantum coherences, such as Bose-Einstein condensation [4–7].

At suitably large atomic densities, about 10^{12} atoms/cm^3, the atom-atom interactions are expected to become important in laser cooling and trapping [8,9]. For far off-resonant lattices, their role can be easily controlled, and one can even consider studying controlled collisions [10], or using the atom-atom interactions to study quantum computing and entanglement [11,12]. Recently it has become possible to make densely occupied far off-resonant lattices [13]. For near-resonant optical lattices, the situation is more complicated, because the main atom-atom effects are light-assisted inelastic collisions, which interfere with the laser-cooling process. Another aspect is that although strong photon scattering leads typically to efficient dissipation and cooling, in suitably dense atomic gases the reabsorption of scattered photons causes also unwanted heating of the atomic cloud. Experimentally the case of densely populated near-resonant lattices has not been studied very much so far, as high occupation densities are hard to produce due to the above-mentioned problems. These problems are present also in basic magneto-optical traps (MOT) so one does not get much gain in density by using a MOT as a preliminary stage.

For near-resonant laser light, we have two situations depending on whether the laser frequency is slightly above the atomic transition (blue-detuned light) or slightly below it (red-detuned light). In the more commonly applied red-detuned case, one obtains the lattice structure rather easily, and can go below the Doppler limit for laser cooling due to the Sisyphus cooling mechanism. For densely populated lattices, this means, however, the above-mentioned appearance of strongly inelastic collisional radiative processes that cause heating and loss of atoms [9].

In this paper, we look at the case of a near-resonant blue-detuned lattice, which is different from the red-detuned case. It is not straightforward to construct a blue-detuned lattice with an efficient cooling mechanism. There are, however, schemes for doing this, based on applying an external magnetic field [14,15], and we have adapted one of them as the basis of our studies. The important benefit of using a near-resonant blue-detuned lattice is that the photon scattering is reduced strongly compared to the red-detuned case. This diminishes the role of photon reabsorption as a heating mechanism, and thus increases the relevance of the light-assisted collisions in the complicated thermodynamics of the atomic cloud.

With blue-detuned light, the nature of the light-assisted collisions is also changed, and instead of strong inelastic processes we have optical shielding of collisions [9]. For weak fields this mechanism is incomplete and can lead to some heating of atoms, but barely to any strong loss. For stronger fields the inelastic contribution disappears, also in the sense that optical shielding forbids close ground-ground encounters which can lead to atom loss or heating, in addition to the light-assisted processes. Optical shielding has been studied both experimentally [16–20] and theoretically [21–23] with laser-cooled atoms in magneto-optical traps, but not, to our knowledge, in optical lattices. None of the theoretical studies so far have treated the cooling process and the shielding process simultaneously.

Thus we expect that, *a priori*, it is better to use blue-detuned lattices for efficient cooling while aiming at an increase in the atomic density in lattices. Matters are, however, complicated by the presence of the Zeeman states with different energies. Also, the mixing of cooling and collisions may produce unexpected effects if the two processes are not separable. Finally, there are indications in previous MOT studies that at very strong fields off-resonant processes can become important. Thus, by using the technique of our earlier study [24,25], we have examined the dynamics of two colliding atoms in a one-dimensional blue-detuned optical

lattice. It turns out that all the above-mentioned aspects, incomplete and complete shielding, and the off-resonant processes, are present also for the blue-detuned lattices. But more importantly, it turns out that the shielding mechanism and the cooling and trapping mechanism can coexist without interfering with each other.

This paper is constructed as follows. First we briefly review in Sec. II the basic properties and construction of blue-detuned optical lattices, and in Sec. III the optical shielding process in collisions. In Sec. IV we present how to treat the two situations within the same dynamical model with Monte Carlo wave-function (MCWF) simulations. The results are given in Sec. V and finally discussed in Sec. VI.

II. BLUE-DETUNED NEAR-RESONANT OPTICAL LATTICES

The light shifts of the sublevels of the atomic ground-state energy states are positive for blue-detuned light. The stronger the coupling, the larger is the light shift, and the higher the level lies in energy. Therefore, the optical potential minima may occur when the atomic ground-state Zeeman sublevel is minimally coupled to the excited states. This implies that it should be possible to trap atoms with laser-field polarization gradients around those points in space where there is no coupling to the excited state. For example, if the ground and excited states have an equal total angular momentum quantum number J, the ground-state sublevel with angular momentum projection state $m_g = J$ is not coupled to the excited state when the light is σ^+ polarized. The coupling strength and the optical potential increase when the atom moves away from the totally dark point, in this case away from the point of σ^+ light polarization.

In the schemes for optical lattices which use, e.g., only one ground- and one excited-state manifold ($J \rightarrow J$), one of the light-shifted eigenstates is in fact a completely dark state which is not coupled to the excited state at any point of space. It would be ideal for trapping atoms but unfortunately the optical potential for this state is flat. This state can be used for efficient laser cooling [26], and the photon scattering is about two orders of magnitude smaller than in other near-resonant laser cooling and trapping schemes. In order to achieve a lattice structure, one can add a magnetic field [14,15], which modifies the energy of the initially flat dark eigenstate in a periodic way. Instead of applying a magnetic field, one can also avoid the flat dark state problem by using two different excited-state hyperfine manifolds [27].

In our study, we consider the magneto-optical $J \rightarrow J$ lattice proposal of Grynberg and Courtois (GC) [14]. The numerical simulations for dynamical collision studies in optical lattices are very demanding [24,25], and the GC scheme allows us to do numerical simulations with parameter values that are also experimentally realistic. We limit our study to the case in which $J_g = J_e = 1$. It is possible to find a level scheme like this in ^{87}Rb, which has $F = 1$ hyperfine states for both the $5S_{1/2}$ ground and for the $5P_{1/2}$ excited state [15]. We label the three ground-state sublevels with $|g_{\pm 1}\rangle, |g_0\rangle$, and the three excited-state sublevels with $|e_{\pm 1}\rangle, |e_0\rangle$, where the integer subscripts indicate the angular momentum projection quantum number m, see Fig. 1. We use the atomic mass of ^{87}Rb in our simulations.

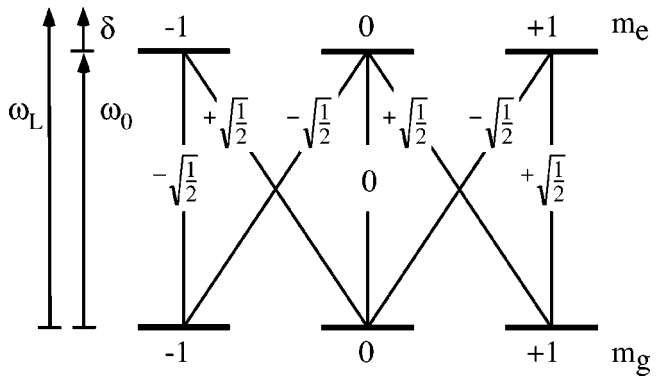

FIG. 1. The level structure of a single atom with the Clebsch-Gordan coefficients of corresponding transitions.

The laser field consists of two counterpropagating beams with orthogonal linear polarizations and with frequency ω_L. For a zero magnetic field, the laser detuning is $\delta = \omega_L - \omega_0$, where ω_0 is the atomic frequency. The total field has a polarization gradient in one dimension and reads (with suitable choices of phases of the beams and origin of the coordinate system)

$$\mathbf{E}(z,t) = \mathcal{E}_0(\mathbf{e}_x e^{ik_r z} - i\mathbf{e}_y e^{-ik_r z}) e^{-i\omega_L t} + \text{c.c.}, \tag{1}$$

where $\mathcal{E}_0$ is the field amplitude and k_r the wave number. With this field, the polarization changes from circular σ^- to linear and then to circular in the opposite direction σ^+ when z changes by $\lambda_L/4$, where λ_L is the wavelength of the laser light.

The intensity of the laser field and the strength of the coupling between the field and the atom are described by the Rabi frequency $\Omega = 2d\mathcal{E}_0/\sqrt{2}\hbar$, where d is the atomic dipole moment of the transition between the ground and excited states. In the level scheme used here, all the allowed transitions are equally strong and the absolute value of the corresponding Clebsch-Gordan coefficient has been included in the definition of the Rabi frequency Ω above.

The magnitude of the light shift is [3] (when taking into account the current level and coupling scheme)

$$U_0 = \tfrac{1}{2}\hbar\,\delta s_0, \tag{2}$$

where s_0 is the saturation parameter given by

$$s_0 = \frac{\Omega^2/2}{\delta^2 + \Gamma^2/4}. \tag{3}$$

The magnetic field $\mathbf{B}$ is applied in the z direction, $B = B_z$, which is also the quantization axis. The ground state $m_g = 0$ is not Zeeman shifted but the states $m_g = \pm 1$ are shifted by $|\mu B| = \hbar\Omega_B$ into opposite directions with respect to each other. Here μ is the magnetic moment along the z axis of the corresponding state. Thus the energy separation between $m_g = \pm 1$ states due to magnetic field is $2\hbar\Omega_B$.

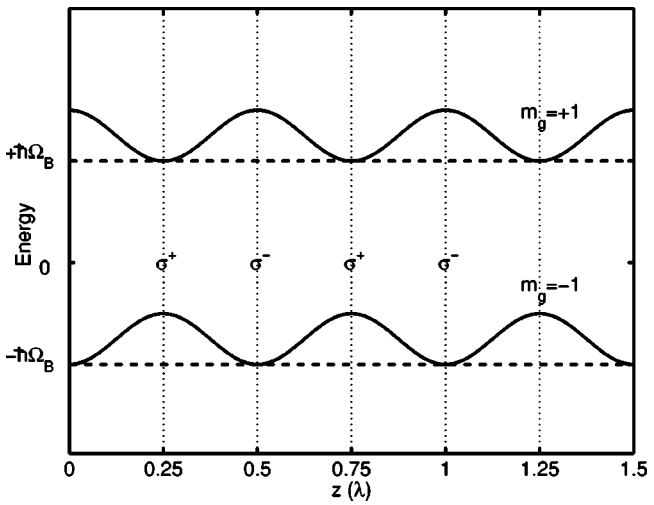

FIG. 2. Schematic view of the optical potentials for the two trapping ground-state Zeeman sublevels. The periodic polarization gradient of the laser field creates the lattice structure and we indicate the points of circular polarizations σ^+ and σ^-. The dashed lines give the Zeeman shifted energy levels which the light field modifies.

If the light shift dominates over the Zeeman shift, $\hbar\Omega_B < U_0$, the lattice is paramagnetic [14]. The atoms are trapped in potential wells located 0.5λ apart, either in the points of σ^+ polarization or in the points of σ^- polarization, depending on the direction of the applied magnetic field. If the Zeeman shift dominates, $U_0 < \hbar\Omega_B$, the eigenstates of the system correspond to Zeeman sublevels onto which the light field induces perturbations. In this case the atoms are trapped in both σ^- and σ^+ light polarization points in space and the lattice behavior is antiparamagnetic [14].

We have done our simulations in the antiparamagnetic regime where the Zeeman shift dominates over light shifts, $U_0 < \hbar\Omega_B$. The polarization gradient of the laser field modifies the lattice potential as in the Sisyphus scheme [3], see Fig. 2. The atoms are cooled by optical pumping, and are trapped into the $m_g = -1$ and $m_g = +1$ ground sublevels. Without the magnetic field there would be no cooling or trapping for the $J_g = J_e = 1$ system due to the dark state and the lack of motional coupling between the dark state and the coupled states [2].

Since the Zeeman shifts for $m_g = -1$ and $m_g = +1$ are in opposite directions, their effective detuning from the resonance is not equal and consequently they experience different optical potential modulation depths U_- and U_+, respectively. The value of U_0 gives the optical potential modulation depth when the Zeeman shift is large compared to the detuning. This is the value that both U_- and U_+ approach when U_0 is kept fixed with increasing detuning. We show the schematic view of optical potentials for ground sublevels in Fig. 2. The relevant lattice properties along with simulation parameters are given in Tables I and II. We have performed a series of simulations for two fixed values of detuning, with a changing Rabi frequency, and another series for a fixed value of U_0, with a changing detuning and Rabi frequency.

TABLE I. Laser parameters for the simulation series with fixed detuning, and the corresponding lattice properties: Detuning δ, Rabi frequency Ω, Zeeman shift Ω_B, lattice modulation depths U_0, U_-, and U_+. The atomic photon recoil energy is $E_r = \hbar^2 k_r^2/2M$, and Γ is the atomic linewidth.

$\delta(\Gamma)$	$\Omega(\Gamma)$	$\Omega_B(\Gamma)$	$U_0(E_r)$	$U_-(E_r)$	$U_+(E_r)$
5.0	1.5	1.25	178	236	143
5.0	2.0	1.25	316	419	254
5.0	3.0	1.25	712	943	572
5.0	5.0	1.875	1980	3120	1447
10.0	2.0	1.25	159	182	141
10.0	4.22	1.875	710	873	599
10.0	8.0	3.125	2554	3704	1948
10.0	10.0	3.75	3990	6359	2905

III. OPTICAL SHIELDING

A. Collisions in the presence of near-resonant light

Two slowly colliding atoms form a quasimolecule. When a laser field is present, the quasimolecule may be resonantly excited at long range at the Condon point R_C where the ground and excited molecular states become resonant. In this case, the nature of the atomic collision depends on the sign of the detuning of the laser [9].

For a red-detuned laser, the excitation is followed by an acceleration of the quasimolecule on an attractive excited state. The collision becomes inelastic when spontaneous decay back to the ground state occurs and the pair of colliding atoms gain kinetic energy. The shared energy increase corresponds to the acceleration on the excited state. This is the radiative heating and escape mechanism. In addition, the atoms may also gain kinetic energy by a fine-structure changing mechanism. If the atom pair survives on the excited state to very small internuclear distances and there is a level crossing between two excited fine-structure states, the pair may change their internal state. When coming out of the collision on a fine-structure state which is asymptotically below the state on which they entered the collision, the kinetic energy of the quasimolecule increases by the corresponding amount. For a review, see Ref. [9].

When the laser field present is blue-detuned, the situation is different. The resonant excitation of the quasimolecule at R_C occurs now to a repulsive molecular state. The atom pair is prevented from approaching close to each other due to the

TABLE II. Laser parameters for the simulation series with fixed lattice depth U_0, and the corresponding lattice properties: Detuning δ, Rabi frequency Ω, Zeeman shift Ω_B, and lattice modulation depths U_0, U_-, and U_+.

$\delta(\Gamma)$	$\Omega(\Gamma)$	$\Omega_B(\Gamma)$	$U_0(E_r)$	$U_-(E_r)$	$U_+(E_r)$
1.5	1.72	0.8125	710	1126	489
5.0	3.0	1.25	712	943	572
7.0	3.54	1.25	712	865	605
10.0	4.22	1.875	710	873	599

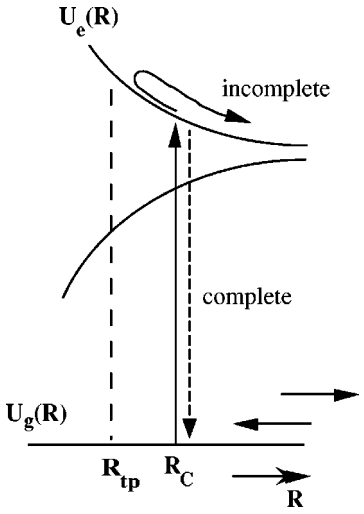

FIG. 3. A schematic semiclassical representation of optical shielding. The quasimolecule is excited resonantly to the repulsive molecular state at the Condon point R_C. Then it reaches the classical turning point R_{tp}, and is finally transferred back to the ground state when arriving at R_C again. If the transfer back to the ground state is not complete, the atom pair may gain kinetic energy as it is further accelerated by the excited-state potential. In this case, shielding is incomplete and the collision is inelastic. If the population transfer between the states is adiabatic, shielding is complete and the collision between the atoms is elastic.

reflection of motion on the repulsive state at the turning point R_{tp}, see Fig. 3. If the transfer of population back to the ground state is not complete when the quasimolecule traverses R_C again, the atom pair may gain kinetic energy. In this case, the shielding is incomplete and the collision is inelastic. If the population transfer between the states is adiabatic and there is no time for spontaneous emission to occur during the process, shielding becomes complete and the laser-assisted collision between atoms is elastic.

It should be noted that despite strong localization of atoms into lattice sites, atoms still move from site to site to some extent. This is due to the finite spatial extent of atomic wave packets and the optical pumping process. Thus the localization does not mean that weak long-distance atom-atom interactions at relatively fixed atom-atom distances now dominate over the more stronger cold collisions between moving atoms.

B. Shielding of ground-state processes

Efficient optical shielding can suppress the rates of unwanted processes which occur at short internuclear distances even in the absence of laser fields [9]. Inelastic ground-ground processes are suppressed because complete shielding simply empties the quasimolecule ground state at R_C and in principle the quasimolecule can never reach the internuclear distances $R<R_C$. Since for near-resonant light the values for R_C are typically hundreds or thousands of angstroms, any small-distance molecular process such as a change of a hyperfine state or Penning ionization is prevented.

In the past, the optical shielding and suppression have been studied experimentally, e.g., in the following contexts: suppression of heating and escape of atoms in MOTs [16], shielding of photoassociative ionizing collisions [17], shielding of ionizing collisions of metastable xenon and krypton [18,19], and optical suppression in two-photon ''energy pooling'' collisions in Rb MOTs [20]. Theoretical methods used for shielding studies include MCWF simulations [21], Landau-Zener [21] and three-dimensional Landau-Zener theory [22], and quantum close-coupling calculations [23]. It should be noted that shielding does not help very much in achieving Bose-Einstein condensation as it involves actual resonant absorption and subsequent emission of photons, with the corresponding recoil momentum effects.

C. Shielding in optical lattices

When studying optical shielding in blue-detuned near-resonant optical lattices, there is no need for additional shielding lasers. The blue-detuned lattice laser itself acts as a shielding laser. Efficient shielding in blue-detuned lattices would make it possible to increase the occupation density even in the case of near-resonant lattices and without the problems arising from light-assisted inelastic collisions and photon reabsorption. This would be in contrast to the case of red-detuned near-resonant optical lattices where the inelastic processes dominate when the occupation density increases and atom-atom interactions are accounted for [24,25].

Our simulation scheme and collision model is similar to the one we have used previously for collision studies in optical lattices; details can be found in Ref. [25]. The simulations require very large computational resources and we note again that we fix the position of one of the two colliding atoms with respect to the lattice. The small number of scattered photons means that in a high-density atom cloud the radiation pressure due to reabsorbed photons decreases. This means that our purely collisional model becomes more realistic in the context of the thermodynamics of the atom cloud, compared to our previous studies of the red-detuned case [24,25].

IV. FRAMEWORK FOR SIMULATIONS

A. Product state basis and Hamiltonian

We formulate the problem in position space and use the two-atom product states [28]. We do not use the adiabatic elimination of the excited states [29] since we want to account for the dynamical nature of atomic interactions in the presence of near-resonant light. The basis vectors are

$$|j_1 m_1\rangle_1 |j_2 m_2\rangle_2, \tag{4}$$

where j_1 and j_2 denote the ground or excited state and m_1, m_2 denote the quantum number for the component of J along the quantization axis z for atoms 1 and 2, respectively, in our $J_g=J_e=1$ system. The total number of states in principle is $6\times 6=36$. In the current coupling and level scheme, it is possible to simplify the problem and use only nine states; see below.

We have to fix the position of one atom, and the binary system wave function depends now only on the position z_2 of the moving atom 2,

$$|\psi(z_2,t)\rangle = \sum_{j_1,j_2,m_1,m_2} \psi^{j_1,m_1}_{j_2,m_2}(z_2,t)|j_1 m_1\rangle_1 |j_2 m_2\rangle_2 . \quad (5)$$

The atomic spatial dimensionality of the problem is reduced from numerically impossible 2 to numerically treatable 1; see Ref. [25] for more discussion. The relative coordinate z between atoms is now $z=z_2-z_f$, where z_f is the position of the fixed atom.

In the atomic product state basis [28], our system Hamiltonian is

$$H_S = H_1 + H_2 + V_{\rm dip} . \quad (6)$$

Here, $V_{\rm dip}$ includes the interaction between the atoms. H_1 and H_2 are the single-atom Hamiltonians for atoms 1 and 2, respectively, in product state space.

The single-atom Hamiltonian for atom α ($\alpha=1,2$) in respective Hilbert spaces is, after the rotating-wave approximation,

$$\tilde{H}_\alpha = \frac{p_\alpha^2}{2M} - \hbar\delta P_{e,\alpha} + \tilde{V}_\alpha + \tilde{U}_\alpha . \quad (7)$$

Here, $P_{e,\alpha} = \Sigma_{m=-1}^{1} |e_m\rangle_\alpha \ {}_\alpha\langle e_m|$, and the interaction between a single atom α and the field is

$$\tilde{V}_\alpha = i\frac{\hbar\Omega}{\sqrt{2}} \sin(kz_\alpha)\{|e_0\rangle_\alpha \ {}_\alpha\langle g_{-1}| + |e_1\rangle_\alpha \ {}_\alpha\langle g_0|\} + \frac{\hbar\Omega}{\sqrt{2}} \cos(kz_\alpha)\{|e_{-1}\rangle_\alpha \ {}_\alpha\langle g_0| + |e_0\rangle_\alpha \ {}_\alpha\langle g_1|\} + \text{H.c.}, \quad (8)$$

where z_α is the position operator of atom α. The dipole-dipole interaction potential $V_{\rm dip}$ is the same as used in Refs. [24] and [25]. The sum over the quantum number m in Eq. (12) of Ref. [25] goes now from $m=-1$ to $m=+1$ for the level scheme $J_g=J_e=1$ studied here.

The interaction of atom α with the magnetic field B in Eq. (7) is

$$\tilde{U}_\alpha = \sum_i m_i \hbar \Omega_{B_i} |i\rangle_\alpha \ {}_\alpha\langle i| , \quad (9)$$

where the sum over i includes all the ground and excited states, and the Zeeman shift factors Ω_{B_i} are for the ground substates $m=\pm 1$ equal to Ω_B, see Tables I and II.

The description of optical shielding is usually given in terms of molecular potentials, see Sec. III. We note that we use the two-atom product state vectors because of their simplicity in treating quantums jumps for the current case. Molecular potentials can be obtained by diagonalizing $V_{\rm dip}$ in Eq. (6).

In the antiparamagnetic regime of the GC optical lattice, the values of detunings are such that the Zeeman shifts are not negligible in all simulations. The $m_g=-1$ level is closer to resonance than the $m_g=+1$ level for the magnetic field orientation we use. Thus the optical potential modulation depth may also be different for the two states. The values of modulation depth U_- and U_+ for levels $m_g=-1$ and m_g+1, respectively, and Zeeman shifts are presented in Tables I and II. In the constant detuning simulations, it is necessary to increase the Zeeman shift when going for stronger laser fields and deeper lattices, in order to stay in the antiparamagnetic regime.

B. Aspects of the simulation method

We use the MCWF method to solve the equation of motion for the density matrix of the two-atom system interacting with semiclassical light fields [8,30,31]. A direct quantum-mechanical solution of the density-matrix master equation by other means is not feasible due to the large size of the density matrix and the coupling of atoms to a large number of vacuum modes of the electric field. The variant of Monte Carlo (MC) methods we use was developed by Dalibard, Castin, and Mølmer [32]. Application of the MCWF method for the study of cold collisions in optical lattices is not straightforward and we have given the details in our earlier publication [25]. As a result of simulations, we obtain a momentum distribution for an atom in the lattice. This distribution is the most informative result when studying optical shielding in the context presented here.

The laser field couples only states where $\Delta m=\pm 1$. The Clebsch-Gordan coefficient between the states $m_g=0$ and $m_e=0$ is zero in the level scheme. It follows that optical pumping rapidly moves population to the ground levels $m_g=\pm 1$, which are coupled only to the excited level $m_e=0$. Thus there is population on only three levels for both of the colliding atoms, the Λ scheme, and the number of the used product state basis vectors can be reduced from 36 to $3\times 3=9$. This simplifies the problem considerably. The simulations take fewer computational resources and are much faster to perform. The dipole-dipole interaction does not change the scheme and it is confirmed by the results of the full simulation, which includes all 36 states. From the molecular potential point of view, this means that only one attractive and one repulsive state is relevant instead of all four different attractive and four different repulsive states.

The number of collisions should be the same for simulations with different parameters for the results to be comparable. The number of collisions is dictated by the number of spontaneously emitted photons. We fix the simulation time to constant value 120, in units of $1/\Gamma s_0$. This guarantees that the average number of spontaneously emitted photons and the number of collisions remains roughly the same for all simulations. We have performed all the simulations for the one-dimensional occupation density of 25% of the lattice, i.e., every fourth lattice site is occupied on average.

V. RESULTS

We present the momentum distributions of three simulation series in Figs. 4, 5, and 6. We do two simulation series with the constant values of detuning δ and changing the Rabi frequency Ω. We have $\delta=5\Gamma$ and $\delta=10\Gamma$ in Figs. 4 and 5, respectively. Figure 6 gives results for a constant optical potential modulation depth, $U_0\sim 710E_r$, and changing δ. We

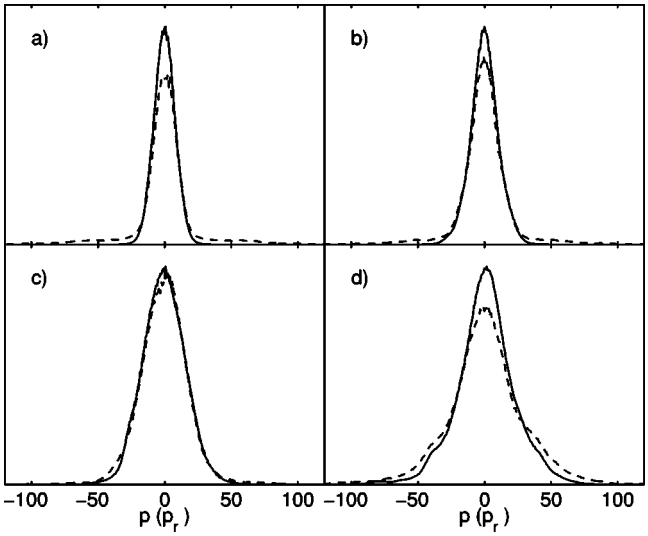

FIG. 4. Momentum probability distributions for the $\delta=5\Gamma$ case. The Rabi frequencies are (a) $\Omega=1.5\Gamma$, (b) $\Omega=2.0\Gamma$, (c) $\Omega=3.0\Gamma$, and (d) $\Omega=5.0\Gamma$. Momentum is expressed in recoil unit $p_r=\hbar k_r$. Dashed line is for interacting and solid line for noninteracting atoms. When Ω increases, the regime changes from incomplete shielding, (a) and (b), to complete shielding, (c), and finally to off-resonant heating in (d). The momentum distributions also get wider due to a deeper lattice with increasing Ω.

compare the results between interacting and noninteracting atoms.

A. Constant detuning

For the smallest values of Ω, the constant detuning simulations show that optical shielding is not complete. Wide

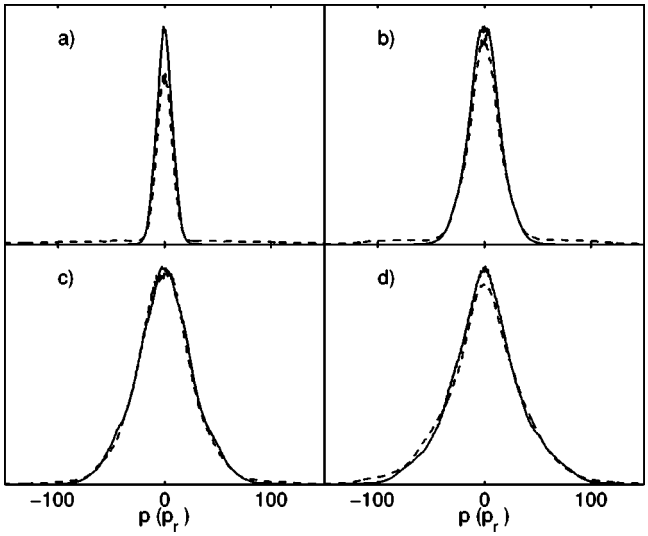

FIG. 5. Momentum probability distributions for the $\delta=10\Gamma$ case. The Rabi frequencies are (a) $\Omega=2.0\Gamma$, (b) $\Omega=4.22\Gamma$, (c) $\Omega=8.0\Gamma$, and (d) $\Omega=10.0\Gamma$. Dashed line is for interacting and solid line for noninteracting atoms. When Ω increases, the regime changes from incomplete shielding, (a) and (b), to complete shielding, (c), and finally to off-resonant effects in (d). The momentum distributions also get wider due to a deeper lattice with increasing Ω.

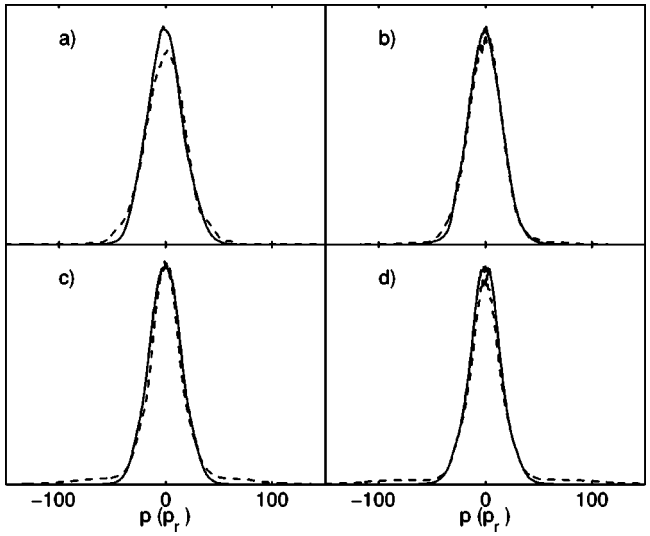

FIG. 6. Momentum distributions for fixed $U_0\sim 710E_r$. (a) $\delta=1.5\Gamma$, (b) $\delta=5.0\Gamma$, (c) $\delta=7.0\Gamma$, and (d) $\delta=10.0\Gamma$. The off-resonant processes play a role at the small detuning, (a). In the intermediate detuning, shielding may become complete and the collisions between atoms are elastic, (b). For larger detuning the shielding is incomplete, (c) and (d).

wings towards large momentum appear [Figs. 4(a), 4(b), 5(a), and 5(b)]. The resonant excitation process at Condon point R_C is not adiabatic and some atoms can move apart on a repulsive molecular state after the collision. If the process terminates for spontaneous decay at $r>R_C$, the atom pair gains a corresponding amount of kinetic energy by acceleration on the repulsive molecular state; see Fig. 3.

The wings get narrower when we increase the value of Ω and they nearly vanish when the point of complete shielding is reached [Figs. 4(c) and 5(c)]. The resonant excitation process for the repulsive state at R_C becomes adiabatic and hardly any change in p distribution is visible when compared to noninteracting atoms. When atoms try to occupy the same lattice site, they collide elastically in this parameter regime.

When we increase the Rabi frequency further, the off-resonant effects come into play [Figs. 4(d) and 5(d)]. The momentum distribution begins to deviate again from the result for noninteracting atoms, and the qualitative character of momentum broadening is now different when compared to the small Ω results. This indicates that the heating process does not arise from incomplete shielding. Additional shoulders that appear in both the interacting and noninteracting cases arise due to the difference in the depth of the two lattice potential wells, $U_{\pm 1}$. When we increase δ, we note that the point of complete shielding moves towards larger U_0, in our case from $\delta=5\Gamma$ and $U_0=712E_r$ to $\delta=10\Gamma$ and $U_0=2554E_r$.

B. Constant lattice depth

Figure 6 shows results for the case of constant optical modulation depth $U_0\sim 710E_r$ and varying detuning. When the detuning is small, the off-resonant effects heat the atomic cloud and small wings appear in momentum distribution; see Fig. 6(a). For an intermediate detuning value, the point of

complete shielding is reached [Fig. 6(b)]. Increasing δ further makes the shielding incomplete and subsequently wide wings appear in the momentum distribution [Figs. 6(c) and 6(d)]. This is in agreement with the study of off-resonant effects of the laser field in cold collisions in MOTs [33]. Keeping the lattice depth constant and increasing the detuning means decreasing the ratio Ω/δ, which reduces the role of off-resonant effects. Simulation studies reported in Ref. [33] show that for collisions in uniform blue-detuned laser fields, the off-resonant effects vanish when Ω/δ decreases until for small values of Ω/δ the shielding effect is again incomplete. This is accordance with the optical lattice results presented here.

VI. CONCLUSIONS

Our simulations demonstrate clearly that optical shielding should be present in blue-detuned near-resonant optical lattices. The shielding process is not expected to always be perfect, but with an appropriate choice of the detuning and the intensity of the trapping laser it is nevertheless possible to strongly suppress the rate of inelastic collisions. For example, with a detuning $\delta=5.0\Gamma$ and a Rabi frequency $\Omega=3.0\Gamma$, giving $U_0=710E_r$ in our scheme, the optical shielding process is practically complete, see Fig. 4(c). If the parameters are not chosen correctly, the shielding process can be either incomplete or reduced by the off-resonant excitation of the quasimolecule states related to attractive atom-atom potentials [33].

We have studied here the antiparamagnetic regime of a GC lattice [14]. In this case, the cooling and trapping mechanism resembles the traditional Sisyphus mechanism [3], making comparisons between our previous study of the red-detuned case more appropriate. In this scheme, the lattice depth depends on the intensity of the laser. The value of detuning for effective shielding increases when the laser intensity and thus the optical potential modulation depth U_0 are increased. Thus for shallow lattices, effective shielding occurs at small detunings, in which case the two trapping potentials are not identical because of the non-negligible Zeeman shift compared to the detuning of the laser.

In the paramagnetic regime of a GC lattice, the lattice depth U_0 is dictated by the strength of the magnetic field more than by the laser intensity. This leaves more freedom for using both the intensity and detuning of the laser to optimize optical shielding for a given lattice depth. This is an interesting subject for possible future studies of collisions in blue-detuned near-resonant optical lattices.

Together with the reduced photon scattering and thus reduced heating of dense atomic clouds by photon reabsorption, optical shielding opens a way to achieve higher occupation densities and lower temperatures in blue-detuned near-resonant optical lattices, compared to the red-detuned case. Unlike in the red-detuned case, two atoms trying to occupy the same lattice site will at worst only repulse each other in an elastic process. It should be noted that optical shielding was originally introduced to, e.g., suppress the hyperfine state changing ground-ground collisions during cooling and trapping of alkali-metal atoms [16], and this additional benefit is naturally present in blue-detuned lattices as well. More importantly, the strong Penning ionization for metastable rare-gas atoms [18,19] should be suppressed as well in blue-detuned lattices. An important benefit here is that all three processes—trapping, cooling, and shielding—are produced by the same set of laser beams.

Considering what is already known about blue-detuned optical lattices, and about optical shielding in magneto-optical traps, our results appear rather obvious. However, they could have been different. Firstly, previous theoretical studies of optical shielding have excluded the actual cooling process [21–23]. Our results show that the two can coexist at least in blue-detuned lattices without apparent problems even in the saturation limit, although the off-resonant excitation of quasimolecule states reduces the shielding efficiency. In experiments in magneto-optical traps, shielding has been implemented typically with an additional catalyst laser, with the red-detuned cooling and trapping lasers either off or on. If the red-detuned cooling and trapping lasers are on, the near-resonant shielding studies become practically impossible due to the strong and usually unfavorable mixing of the two processes [19]. In other words, we hope that our work serves as a motivation for experimentalists to perform shielding studies in near-resonant blue-detuned lattices in the presence of the cooling process. Although the densities that have been available so far have been rather low, the use of, e.g., metastable rare-gas atoms could provide useful information due to the clear ion signal that marks collision events [18].

Secondly, very few theoretical studies of shielding with near-resonant light have been done so far, as the interest has been mostly on the large-detuned laser fields. This is because the theoretical treatment is simplified when we can ignore the spontaneous emission (at large detunings, the excited-state potential is so steep that the resulting fast dynamics and slow spontaneous emission decouple trivially from each other). In an earlier near-resonant study [33], the possibility of spontaneous emission from the excited repulsive quasimolecule state during the slow-down of the relative motion of the two atoms was found to be suppressed by reexcitation, until the atoms had finally turned around, i.e., the efficiency of shielding increased without limit with laser intensity. Similarly, in our study there does not seem to be any evidence for breakdown of efficient shielding due to such a spontaneous-emission effect.

Thirdly, experiments show clearly that the shielding efficiency of inelastic ground-ground collisions can saturate to some finite value as we increase the laser intensity [18,19]. The reason for this is still unclear. It has been attributed to various processes, in addition to the above-mentioned premature termination of shielding via spontaneous emission [21]. Other possibilities include counterintuitive or off-resonant processes involving different partial waves or other processes that similarly involve multiple states (in contrast to the basic two-state approaches [9,19,22,23]), or off-resonant excitation to the attractive molecular states [18]. We find that off-resonant excitation is indeed present in our studies, where $\delta\leqslant 10\Gamma$, i.e., our detuning is small in general and comparable to the Rabi frequencies. This is in agreement with the much more simplified three-state study done earlier

[33]. When $\Omega/\delta \gg 1$, the steady-state formation can surpass the dynamical resonant excitation process at suitably low collision velocities, and we see that indeed it is the near-zero region of the momentum distribution that gets depleted in Fig. 4(d), and not the near-average velocity region as in the red-detuned lattice case. However, as discussed before, this off-resonant process cannot explain the observed saturation of shielding, as that happens at very large detunings, for which $\Omega/\delta \ll 1$, but Ω is large enough for the situation to correspond mainly to Fig. 4(c), the case of complete shielding. There is no evidence of saturation of shielding in our studies, but due to the limitations of our model (one dimension only, and ignoring the very small scale molecular processes), we cannot state conclusively that it would not be present in any experiments.

Due to the limitations set by the numerics, we have considered only the one-dimensional case where the direction of propagation for the lattice laser beams and the direction of the collision axis are the same. In practice, even in a one-dimensional lattice the collision axis is still in a three-dimensional space and can have any angle with respect to the beam propagation and electric field directions. In our previous study [25], we report the result of the full calculation of the dipole coupling term for two atoms. Basically, the result shows that for any collision angle the interaction between the colliding atoms remains qualitatively the same, with a number of attractive and repulsive molecular potentials (this situation, by the way, is behind the reason why a possible angle dependence cannot really be used to explain the saturation of shielding in xenon; see Ref. [19]). Thus one can expect that also for fully three-dimensional collisions in blue-detuned near-resonant lattices, the coexistence of cooling and shielding is possible. Interestingly, this also implies that for a one-dimensional lattice we have cooling and localization to lattice sites only in one direction, but the shielding effect induced by the lattice beams should nevertheless be present for all directions of the collision axis, including the case where this axis is perpendicular to the lattice direction.

Thus, we have demonstrated that efficient optical shielding should be possible in near-resonant blue-detuned optical lattices. More precisely, it is mediated by the trapping and cooling lasers themselves but it does not interfere with the cooling process, unlike in basic magneto-optical traps created with strong red-detuned lasers. Especially, we have theoretically demonstrated optical shielding within a level scheme, which is more complicated (and realistic) than the two-state models used so far [9,21]. Our approach is fully quantum, takes spontaneous emission into account, and is applicable even for strong fields. Finally, our results show that by a suitable choice of lattice parameters it should be possible to obtain efficient cooling and trapping, together with efficient optical shielding of collisional processes, and yet to avoid any contributions from off-resonant excitation to the attractive quasimolecule states.

ACKNOWLEDGMENTS

We thank Kirstine Berg-Sørensen for helpful discussions. J.P. and K.-A.S. acknowledge the Academy of Finland (Projects 43336 and 50314) and the European Union IHP CAUAC Project for financial support, and the Finnish Center for Scientific Computing (CSC) for computing resources. J.P. acknowledges support from the National Graduate School on Modern Optics and Photonics.

[1] H.J. Metcalf and P. van der Straten, *Laser Cooling and Trapping* (Springer, Berlin, 1999).

[2] P.S. Jessen and I.H. Deutsch, Adv. At., Mol., Opt. Phys. **37**, 95 (1996); D.R. Meacher, Contemp. Phys. **39**, 329 (1998); S. Rolston, Phys. World **11**(10), 27 (1998); L. Guidoni and P. Verkerk, J. Opt. B: Quantum Semiclassical Opt. **1**, R23 (1999).

[3] J. Dalibard and C. Cohen-Tannoudji, J. Opt. Soc. Am. B **6**, 2023 (1989); P.J. Ungar, D.S. Weiss, E. Riis, and S. Chu, *ibid.* **6**, 2058 (1989).

[4] W.K. Hensinger, H. Häffner, A. Browaeys, N.R. Heckenberg, K. Helmerson, C. McKenzie, G.J. Milburn, W.D. Phillips, S.L. Rolston, H. Rubinsztein-Dunlop, and B. Upcroft, Nature (London) **412**, 52 (2001).

[5] M. Greiner, O. Mandel, T. Esslinger, T.W. Hänsch, and I. Bloch, Nature (London) **415**, 39 (2002).

[6] S. Burger, F.S. Cataliotti, C. Fort, F. Minardi, M. Inguscio, M.L. Chiofalo, and M.P. Tosi, Phys. Rev. Lett. **86**, 4447 (2001); P. Pedri, L. Pitaevskii, S. Stringari, C. Fort, S. Burger, F.S. Cataliotti, P. Maddaloni, F. Minardi, and M. Inguscio, *ibid.* **87**, 220401 (2001).

[7] O. Morsch, J.H. Müller, M. Cristiani, D. Ciampini, and E. Arimondo, Phys. Rev. Lett. **87**, 140402 (2001).

[8] M.J. Holland, K.-A. Suominen, and K. Burnett, Phys. Rev. Lett. **72**, 2367 (1994); Phys. Rev. A **50**, 1513 (1994).

[9] K.-A. Suominen, J. Phys. B **29**, 5981 (1996); J. Weiner, V.S. Bagnato, S. Zilio, and P.S. Julienne, Rev. Mod. Phys. **71**, 1 (1999) and references therein.

[10] D. Jaksch, C. Bruder, J.I. Cirac, C.W. Gardiner, and P. Zoller, Phys. Rev. Lett. **81**, 3108 (1998).

[11] G.K. Brennen, C.M. Caves, P.S. Jessen, and I.H. Deutsch, Phys. Rev. Lett. **82**, 1060 (1999); G.K. Brennen, I.H. Deutsch, and P.S. Jessen, Phys. Rev. A **61**, 062309 (2000); I.H. Deutsch, G.K. Brennen, and P.S. Jessen, Fortschr. Phys. **48**, 925 (2000).

[12] D. Jaksch, H.-J. Briegel, J.I. Cirac, C.W. Gardiner, and P. Zoller, Phys. Rev. Lett. **82**, 1975 (1999); H.-J. Briegel, T. Calarco, D. Jaksch, J.I. Cirac, and P. Zoller, J. Mod. Opt. **47**, 415 (2000).

[13] M.T. DePue, C. McCormick, S.L. Winoto, S. Oliver, and D.S. Weis, Phys. Rev. Lett. **82**, 2262 (1999); A.J. Kerman, V. Vuletić, C. Chin, and S. Chu, *ibid.* **84**, 439 (2000).

[14] G. Grynberg and J.-Y. Courtois, Europhys. Lett. **27**, 41 (1994); K.I. Petsas, J.-Y. Courtois, and G. Grynberg, Phys. Rev. A **53**, 2533 (1996).

[15] A. Hemmerich, M. Weidemüller, T. Esslinger, C. Zimmermann, and T. Hänsch, Phys. Rev. Lett. **75**, 37 (1995).

[16] S. Bali, D. Hoffmann, and T. Walker, Europhys. Lett. **27**, 273

(1994); V. Sanchez-Villicana, S.D. Gensemer, K.Y.N. Tan, A. Kumarakrishnan, T.P. Dinneen, W. Süptitz, and P.L. Gould, Phys. Rev. Lett. **74**, 4619 (1995); S.R. Muniz, L.G. Marcassa, R. Napolitano, G.D. Telles, J. Weiner, S.C. Zilio, and V.S. Bagnato, Phys. Rev. A **55**, 4407 (1997).

[17] L. Marcassa, S. Muniz, E. de Queiroz, S. Zilio, V. Bagnato, J. Weiner, P.S. Julienne, and K.-A. Suominen, Phys. Rev. Lett. **73**, 1911 (1994).

[18] H. Katori and F. Shimizu, Phys. Rev. Lett. **73**, 2555 (1994); M. Walhout, U. Sterr, C. Orzel, M. Hoogerland, and S.L. Rolston, *ibid.* **74**, 506 (1995).

[19] K.-A. Suominen, K. Burnett, P.S. Julienne, M. Walhout, U. Sterr, C. Orzel, M. Hoogerland, and S.L. Rolston, Phys. Rev. A **53**, 1678 (1996).

[20] C.I. Sukenik, D. Hoffmann, S. Bali, and T. Walker, Phys. Rev. Lett. **81**, 782 (1998).

[21] K.-A. Suominen, M.J. Holland, K. Burnett, and P.S. Julienne, Phys. Rev. A **51**, 1446 (1995).

[22] V.A. Yurovsky and A. Ben-Reuven, Phys. Rev. A **55**, 3772 (1997).

[23] R. Napolitano, J. Weiner, and P.S. Julienne, Phys. Rev. A **55**, 1191 (1997).

[24] J. Piilo, K.-A. Suominen, and K. Berg-Sørensen, J. Phys. B **34**, L231 (2001).

[25] J. Piilo, K.-A. Suominen, and K. Berg-Sørensen, Phys. Rev. A **65**, 033411 (2002).

[26] M. Weidemüller, T. Esslinger, M.A. Ol'Shanii, A. Hemmerich, and T. Hänsch, Europhys. Lett. **27**, 109 (1994).

[27] H. Stecher, H. Ritsch, P. Zoller, F. Sander, T. Esslinger, and T.W. Hänsch, Phys. Rev. A **55**, 545 (1997).

[28] C. Cohen-Tannoudji, B. Diu, and F. Laloë, *Quantum Mechanics* (Wiley-Interscience, Paris, 1977), Vol. I, Chap. II F.

[29] K.I. Petsas, G. Grynberg, and J.-Y. Courtois, Eur. Phys. J. D **6**, 29 (1999), and references therein.

[30] B. Garraway and K.-A. Suominen, Rep. Prog. Phys. **58**, 365 (1995), and references therein.

[31] K.-A. Suominen, Y.B. Band, I. Tuvi, K. Burnett, and P.S. Julienne, Phys. Rev. A **57**, 3724 (1998).

[32] J. Dalibard, Y. Castin, and K. Mølmer, Phys. Rev. Lett. **68**, 580 (1992); K. Mølmer, Y. Castin, and J. Dalibard, J. Opt. Soc. Am. B **10**, 524 (1993).

[33] K.-A. Suominen, K. Burnett, and P.S. Julienne, Phys. Rev. A **53**, R1220 (1996).